Inorganic Chemistry
Article
pubs.acs.org/IC

Molecular versus Ionic Structures in Adducts of GaX_3 with Monodentate Carbon-Based Ligands

Ahmad El-Hellani, Julien Monot, Régis Guillot, Christophe Bour, and Vincent Gandon*

ICMMO (UMR CNRS 8182), Université Paris-sud, 91405 Orsay Cedex, France

Ⓢ *Supporting Information*

ABSTRACT: A molecular donor−acceptor adduct has been isolated by the reaction of the *N*-heterocyclic carbene 1,3-dimethyl imidazol-2-ylidene (diMe-IMD) with $GaCl_3$. In contrast, the structurally related, yet much more nucleophilic, 1,3-dimethyl-2-methylene-2,3-dihydro-1*H*-imidazole (diMe-MDI) gave rise to ion pairs of type $[L_2GaX_2][GaX_4]$, where X = Cl, Br, or I. With $IBioxMe_4$, a *N*-heterocyclic carbene that is more nucleophilic than diMe-IMD, the outcome of the reaction was dependent on the nature of the halide. Ionic 1:1 adducts between monodentate ligands and GaX_3 salts have only one precedent in the literature. The peculiar behavior of carbon-based ligands was explained on the basis of their electronic properties and reaction kinetics.

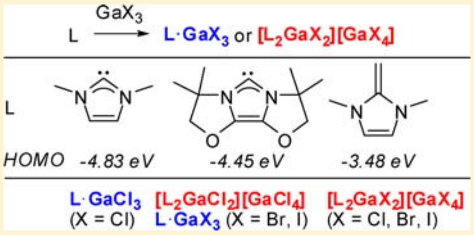

INTRODUCTION

It is well-known that the reaction of Group 13 hydrides, alkyls, and halides (MX_3, where M is a Group 13 element and X = H, alkyl, halogen) with Lewis bases gives adducts of type $MX_3{\cdot}L$ and $M_2X_6{\cdot}2L$ (1:1 ratio), or adducts of type $MX_3{\cdot}2L$ and $M_2X_6{\cdot}4L$ (1:2 ratio; see Scheme 1).[1] With boron, only 1:1 adducts have been thus far reported.[1] The first $M_2X_6{\cdot}2L$ complex $B_2H_6{\cdot}2NH_3$ was reported in 1923.[2] Its structure, elucidated by Parry in 1958, consists of an ion pair of formula $[(NH_3)_2BH_2][BH_4]$.[3] Such compounds are commonly formed in reactions of boron hydride and halides with amines, especially bidentate ones, imines, iminophosphanes, derivatives of urea, and acetonitrile. With other Group 13 elements, most reported 1:1 adducts are molecular species, even with bidentate ligands, except those preorganized for chelation.[4] Only rare examples are known with monodentate ligands. With aluminum, $[(THF)_2AlCl_2][AlCl_4]$ and the corresponding bis(diisopropylamino)phosphaneimine complex have been described.[5] For gallium, only $[(Me_3PO)_2GaI_2]GaI_4$ has been characterized.[6] To the best of our knowledge, no examples have been reported with indium and thallium. In fact, with monodentate amines, ethers, nitriles, and phosphine oxides, the heavier congeners of boron instead give rise to 1:2 adducts of type $MX_3{\cdot}2L$ or $[L_4MX_2][MX_4]$.[7]

Scheme 1. Known Structures of Molecular (A, C) and Ionic (B, D, E) Complexes of Group 13 MX_3 Salts (X = Hydride, Alkyl, Halide; Coordinated Atom of L: C, N, O, P, S, As, Se, Te)

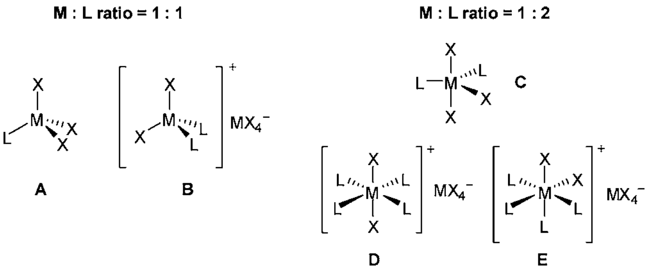

The selectivity between molecular adducts and ion pairs is not yet understood as well. Only two mechanistic studies leading to contrasting results have been published so far. The first one concerned bidentate ligands.[8] DFT computations led to the conclusion that the molecular complexes $M_2X_6{\cdot}en$ and $M_2X_6{\cdot}tmen$ (M = Al, Ga; X = H, Me, Cl, Br, I; en = ethylenediamine; tmen = tetramethylethylenediamine) are always more stable in the gas phase than the corresponding ion pairs. However, ion pairs were systematically characterized by X-ray diffraction. This led the authors to suggest that the formation of ionic assemblies in the condensed phase is due to the establishment of noncovalent interactions (ion−ion interaction and hydrogen bonds). Thus, the selectivity is believed to be thermodynamic in origin. In contrast, the mechanism that was proposed to account for the formation of $[(NH_3)_2BH_2][BH_4]$ from B_2H_6 and NH_3 relies on kinetic arguments (Scheme 2).[9] After nucleophilic addition of a first equivalent of ammonia to diborane to give $H_3NBH_2(\mu\text{-}H)BH_3$, one or several units of $BH_3{\cdot}NH_3$ form an adduct through dihydrogen and hydrogen bonds in which the unsaturated boron B^2 becomes sterically hindered. Consequently, the second equivalent of ammonia adds faster to the already complexed boron B^1, giving rise to an ion pair. Only a catalytic amount of $BH_3{\cdot}NH_3$ is required to achieve this transformation.

Group 13 donor−acceptor complexes are enjoying increasing use in organic synthesis and catalysis.[10,11] They can also be used to activate small molecules,[12] and they are promising

Received: November 8, 2012
Published: December 20, 2012

Scheme 2. Formation Mechanism of the Diammoniate of Diborane

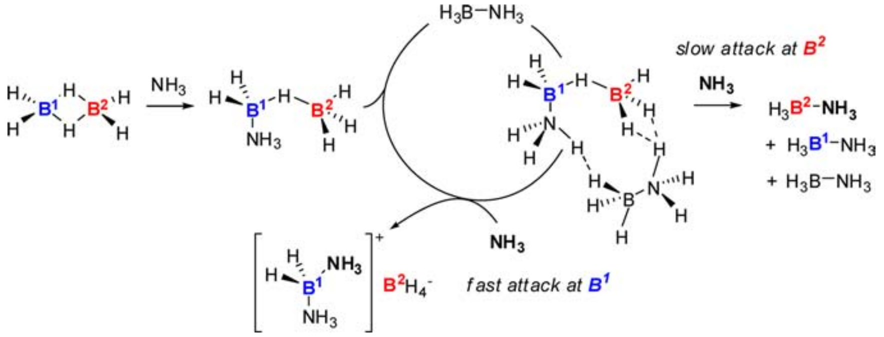

compounds for hydrogen storage applications.[13] Therefore, it is of prime importance to understand the factors governing the structure of these species. A recent paper dealing with In(III)-catalyzed carbocyclization of enynes clearly illustrates this matter (Scheme 3). Whereas $InCl_3$ was believed to be the active species, detailed analysis of the mechanism implicated $InCl_2^+$. The latter was detected by mass spectroscopy, probably bonded to the *gem*-diester tether of the enyne system or of the reaction product.[14] Other reports highlight the formation of active cations derived from molecular Lewis acids, such as $[L_2AlCl_2]^+$ or $[L_2AlMe_2]^+$ from $[Me_2AlCl]_2$.[15]

Scheme 3. In(III)-Catalyzed Cycloisomerization of a 1,6-enyne[a]

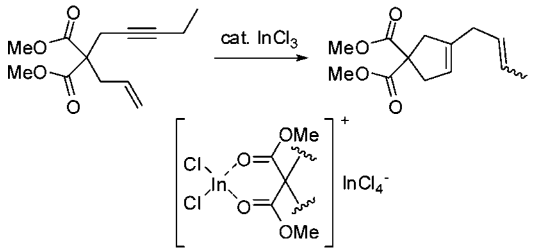

[a] $InCl_2^+$ is the active species.

Following our work on donor−acceptor adducts of gallium halides with *N*-heterocyclic carbenes,[16] we report that not only molecular species but also ion pairs can be formed in this series, even with monodentate ligands. We have studied the two rationales discussed above and devised a kinetic scenario, taking the electronic properties of the ligands into account.

■ EXPERIMENTAL SECTION

General. All reactions were performed in oven-dried flasks under a positive pressure of argon. Commercially available reagents were used as received without further purification. Gallium(III) halides were obtained from Alfa Aesar. Hexane and dichloromethane were distilled from calcium hydride, diethyl ether, and tetrahydrofuran (THF) were distilled from sodium/benzophenone ketyl. ^1H and ^{13}C NMR spectra were recorded on AM250, AV300, AV360, DRX400 MHz Bruker spectrometers. Chemical shifts are given in units of ppm. The spectra were calibrated to the residual ^1H and ^{13}C signals of the solvent. ^{71}Ga (122.0 MHz) NMR spectra were recorded on a Bruker DRX400 and referenced to $[Ga(H_2O)_6]^{3+}$. Data are represented as follows: chemical shift, multiplicity (s = singlet, d = doublet, b = broad), coupling constant (*J*, in Hz), and integration. High-resolution mass spectroscopy (HRMS) were performed on a MicrOTOFq Bruker spectrometer.

Synthesis of 1. 1,3-Dimethylimidazolium iodide (2.2 mmol) was suspended in dry THF (34 mL) and *t*BuOK (2.2 mmol) was added at room temperature (rt) in one portion. The suspension was stirred for 45 min. The mixture was filtered and cooled to −25 °C. Gallium trichloride (2.2 mmol) was added in one portion and the reaction mixture was stirred overnight at rt. The clear solution was then evaporated and ethanol was added to precipitate the complex. After filtration, the gallium complex was obtained as a white solid. Yield: 81%, mp 88−90 °C. ^1H NMR (360 MHz, THF-d_8) δ 7.44 (s, 2 H), 4.07 (s, 6 H). ^{13}C NMR (90 MHz, THF-d_8) δ 125.5, 38.1. ^{71}Ga NMR (122.0 MHz, THF-d_8) δ 263 (bs). HRMS (ESI) *m/z*: Calcd for $C_5H_8Cl_2GaN_2$ $[M-Cl]^+$: 234.9315; Found: 234.9329. Single crystals were grown in THF by slow evaporation.[17]

Synthesis of 2−4. To a solution of 1,3-dimethyl-2-methylene-2,3-dihydro-1*H*-imidazole[18] (0.5 mmol) in THF (7 mL) was added gallium(III) chloride (0.5 mmol) in one portion at −25 °C. The cooling bath was removed, and the reaction mixture was stirred for 12 h, during which a white powder precipitated. The complex was isolated after filtration and washings with THF. (**2**) Yield: 70%, beige powder, mp 62 °C. ^1H NMR (300 MHz, CD_2Cl_2) δ 6.99 (d, *J* = 3.9 Hz, 2 H), 3.78 (s, 6 H), 2.51 (s, 2 H). ^{13}C NMR (75 MHz, THF-d_8) δ 151.2, 120.7, 120.4, 35.6. ^{71}Ga NMR (122 MHz, THF-d_8) δ 249 (s). HRMS (ESI+) *m/z*: Calcd for $C_{12}H_{20}Cl_2GaN_4$ $[M]^+$: 359.0315, Found: 359.0310 ; HRMS (ESI−) *m/z*: Calcd for $GaCl_4$ $[M]^-$: 208.8010, Found: 208.8018. (**3**) Yield: 85%, beige powder, mp 89 °C. ^1H NMR (250 MHz, THF-d_8) δ 7.26 (s, 2 H), 3.82 (s, 6 H), 2.76 (s, 2 H). ^{13}C NMR (75 MHz, THF-d_8) δ 153.0, 122.4, 36.5. ^{71}Ga NMR (122 MHz, THF-d_8) δ 58 (s). HRMS (ESI+) *m/z*: Calcd for $C_{12}H_{20}Br_2GaN_4$ $[M]^+$: 446.9305, Found: 446.9294; HRMS (ESI−) *m/z*: Calcd for $GaBr_4$ $[M]^-$: 384.5989, Found: 384.6019. (**4**) Yield: 85%, white powder, mp 108−110 °C. ^1H NMR (300 MHz, $CDCl_3$) δ 7.31 (s, 2 H), 3.90 (s, 6 H), 2.81 (s, 2 H). ^{13}C NMR (75 MHz, THF-d_8) δ 153.8, 122.3, 37.1. ^{71}Ga NMR (122.0 MHz, CD_2Cl_2) δ −465 ppm (s). HRMS (ESI+) *m/z*: Calcd for $C_{12}H_{20}I_2GaN_4$ $[M]^+$: 542.9028, Found: 542.9008; HRMS (ESI−) *m/z*: Calcd for GaI_4 $[M]^-$: 576.5435, Found: 576.5438. Single crystals were grown by slow diffusion of diethyl ether to a dichloromethane solution of the gallium complex.[17]

Synthesis of 5−7. To a solution of IBioxMe$_4$-OTf[19] (0.27 mmol) in dry THF (3 mL) was added potassium *tert*-butoxide (*t*BuOK, 0.33 mmol) in one portion at rt. The reaction was stirred for 40 min at rt, filtered, and evaporated under vacuum. The residue was suspended in hexane and the gallium(III) halide (0.33 mmol) was added at rt. The reaction mixture was stirred overnight at rt. The solvent was evaporated and the residue was dissolved in a small amount of dichloromethane. Diethyl ether was added to precipitate the remaining imidazolium salt, which was removed by filtration. After evaporation, the gallium complex was obtained as a solid. (**5**) Yield: 84%, gray crystals, mp 120−122 °C. ^1H NMR (250 MHz, CD_2Cl_2) δ 4.71 (s, 8 H), 1.78 (s, 24 H). ^{13}C NMR (100 MHz, CD_2Cl_2) δ 128.5, 126.1, 110.5, 88.8, 88.4, 67.6, 65.7, 26.0, 25.9. ^{71}Ga NMR (122.0 MHz, CD_2Cl_2) δ 249 ppm. HRMS (ESI) *m/z*: Calcd for $C_{22}H_{32}Cl_2GaN_4O_4$ $[M^+]$: 555.1051; Found: 555.1042. (**6**) Yield: 17%, yellow solid, mp 170−173 °C. ^1H NMR (250 MHz, CD_2Cl_2) δ 4.59 (s, 4 H), 1.95 (s, 12 H). ^{13}C NMR (75 MHz, $CDCl_3$) δ 126.9, 88.6, 66.3, 25.7. MS (ESI) *m/z*: Calcd for $C_{11}H_{16}Br_2GaN_2O_2$ $[M-Br]^+$: 434.88; Found: 434.90. (**7**) Yield: 47%, light brown solid, mp 159−161 °C. ^1H NMR

(250 MHz, CD_2Cl_2) δ 4.58 (s, 4 H), 2.07 (s, 12 H). ^{13}C NMR (100 MHz, $CDCl_3$) δ 126.5, 88.6, 66.8, 26.2. HRMS (ESI) *m*/*z*: Calcd for $C_{11}H_{16}GaI_2N_2O_2$ $[M-I]^+$: 530.8551; Found: 530.8550. Single crystals obtained from CH_2Cl_2 by slow evaporation.[17]

■ COMPUTATIONAL DETAILS

Geometry optimizations were carried out using the Gaussian 03 software package[20] at the BP86[21]/def2-TZVPP[22] level of theory. Stationary points were characterized as minima by calculating the Hessian matrix analytically at this level of theory. Thermodynamic corrections were taken from these calculations. The standard state for all thermodynamic data is 298.15 K and 1 atm. For dimeric compounds and ion pairs, counterpoise calculations were achieved to obtain the BSSE correction at the BP86/def2-TZVPP level.[23] Solvation corrections for THF were computed at the BP86/def2-TZVPP level, using the polarizable continuum model (PCM) with UFF radii using the gas-phase optimized structures.[24] Single-point energies at the BP86/def2-TZVPP-optimized geometries were calculated using the ab initio method MP2[25]/def2-TZVPP. Only the MP2 energies (*E*) and Gibbs free energies (*G*) are discussed. The latter include counterpoise correction when appropriate. When solvation correction has been applied, *G* becomes *G*solv.

■ RESULTS AND DISCUSSION

All 1:1 adducts of GaX_3 in any monodentate ligand series reported so far are molecular of type $GaX_3{\cdot}L$, except in one case. With trimethylphosphine oxide, and in striking contrast with monodentate phosphines (and even flexible diphosphines), the ion pair $[(Me_3PO)_2GaI_2]GaI_4$ was isolated.[6] Since phosphine oxides are more nucleophilic than phosphines, we wondered whether this distinct behavior could be attributed to the electronic properties of the ligand. Unlike adducts of GaX_3 with *N*-heterocyclic carbenes, phosphine complexes are quite unstable to air and moisture.[26] Therefore, we focused our study on the former category, which has already found applications in catalysis.[16] Well-defined *N*-heterocyclic carbene adducts of Group 13 trihalides have been described.[27] With aluminum[28] and gallium,[16,29] molecular 1:1 complexes have been crystallographically characterized. This is also true for non-*N*-heterocyclic carbenes.[30] Similarly, the reaction of NHCs with indium[31] and thallium trihalides[32] produces molecular 1:1 adducts, but also molecular 1:2 adducts.

1,3-Dimethyl imidazol-2-ylidene (diMe-IMD) was generated in situ from the corresponding imidazolium iodide and reacted with $GaCl_3$ in THF as shown in Scheme 4.

Scheme 4. Synthesis of (diMe-IMD)$GaCl_3$ (1)

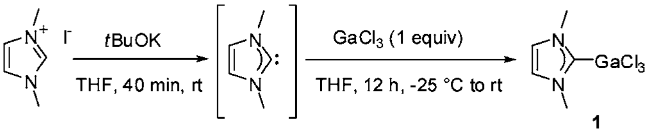

Single crystals of this unprecedented complex were grown directly from this solution. In the solid state, the resulting complex **1** is molecular, as shown by X-ray crystallography (Figure 1). The geometrical features of this compound are similar to those of previously reported (NHC)$GaCl_3$ adducts (see Table S2 in the Supporting Information).[29a] Inspection of the crystal packing shows, as one would expect, that the different units are bound by H-bonds between the Cl atoms, the CH_3 groups, and the vinylic hydrogens.[33]

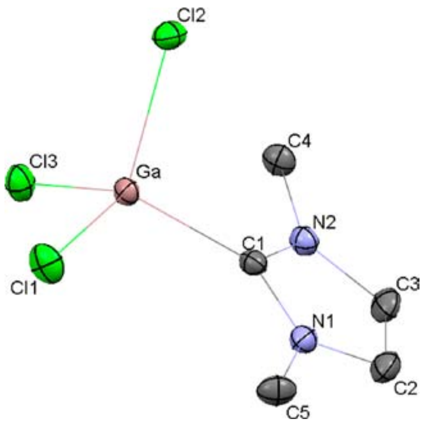

Figure 1. Crystal structure of **1** (thermal ellipsoids at 50% probability level; hydrogen atoms omitted for the sake of clarity).

There is no transformation of this adduct into the corresponding ion pair in solution. The THF solution of **1** was studied by ^{71}Ga NMR. A single broad peak at δ 263 ppm was observed, which is typical for a gallium center in a C_{3v} environment.[4a] The sharp singlet of $GaCl_4^-$ at 249 ppm could not be detected, at least with a fresh sample. With time, the signal of $GaCl_4^-$ appeared but was due to the formation of the hydrolysis product [diMe-IMDH][$GaCl_4$]. As a general rule, no equilibration between the two possible species has been reported for any $GaX_3{\cdot}NHC$ complex, even in chlorinated solvents.[29]

1,3-Dimethyl-2-methylene-2,3-dihydro-1*H*-imidazole (diMe-MDI) is structurally close to the diMe-IMD carbene. It is a strong donor ligand,[34] as shown by the average CO stretching wavenumber of 2003 cm^{-1} for (diMe-MDI)$Rh(CO)_2Cl$.[18] Its reaction with $GaCl_3$ was performed under the same experimental conditions that were used with diMe-IMD (Scheme 5). This time, a large amount of insoluble material was collected.

Scheme 5. Synthesis of $[(diMe\text{-}MDI)_2GaX_2]GaX_4$ (2–4)

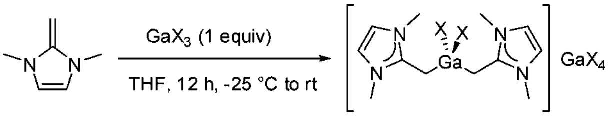

2 (X = Cl)
3 (X = Br)
4 (X = I)

The precipitate was crystallized from a CH_2Cl_2 solution after slow diffusion of Et_2O. X-ray structure analysis revealed the ionic nature of **2** (Figure 2; see also Table S3 in the Supporting Information). The crystal packing showed a network of H-bonds between the Cl atoms of the $GaCl_2^+$ fragment and vinylic hydrogens.[33] Moreover, the $GaCl_4^-$ ion of one unit sits on an imidazolium ring of another unit, as a consequence of Coulombic interaction.[35] ^{71}Ga NMR of **2** in CH_2Cl_2 did not show a signal corresponding to a molecular adduct; only the sharp peak of $GaCl_4^-$ was observed (δ 249 ppm). As is usually the case in such assemblies, the gallium nucleus of the cationic moiety could not be detected.[4a]

The formation of ion pairs is normally facilitated when ions are of small size. However, with diMe-MDI, ion pairs were also

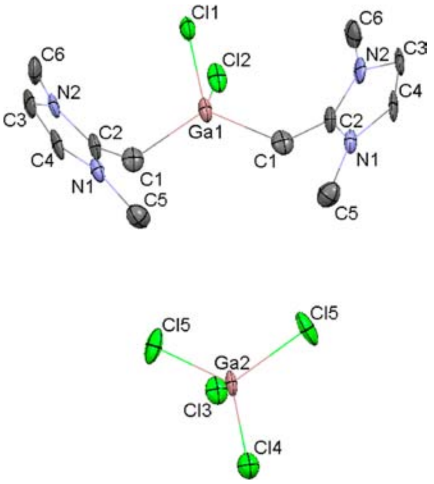

Figure 2. Crystal structure of **2** (thermal ellipsoids at 50% probability level; hydrogen atoms omitted for the sake of clarity).

obtained with the larger $GaBr_4^-$ (**3**) and GaI_4^- (**4**) ions. These complexes could not be characterized by X-ray diffraction but ^{71}Ga NMR ($GaBr_4^-$, δ 58 ppm; GaI_4^-, δ −465 ppm) and HRMS analyses left no doubt concerning the structural assignment.

The relative solubilities of **1** and **2** raise two questions. While complex **1** is soluble in THF (from which single crystals were grown), complex **2** precipitates from this solvent (single crystals were grown in CH_2Cl_2). Therefore, one may wonder whether molecular adducts are formed in THF in both cases, from $GaCl_3{\cdot}THF$,[36] in which case the conversion of **2** into an ion pair might be due to a solvent effect. The second question concerns the steric hindrance created by diMe-IMD, compared to diMe-MDI. Indeed, diMe-IMD has a $\%V_{bur}$ of 26.1 and diMe-MDI of 18.7.[37] On the basis of the reaction of IBioxMe$_4$[19] with $GaCl_3$, these two hypotheses seem quite unconvincing. First, ion pair **5** was obtained either in hexane or in THF (Scheme 6). Therefore, an ion pair can be obtained perfectly in THF, even though Ga_2Cl_6 is instantaneously cleaved into monomeric $GaCl_3{\cdot}THF$. This result is in agreement with the reaction of NH_3 with B_2H_6 or $BH_3{\cdot}THF$, giving both $[(NH_3)_2BH_2][BH_4]$, albeit as a side-product in the latter case.[9] Second, IBioxMe$_4$ is much more sterically demanding than diMe-IMD, its $\%V_{bur}$ being of 30.2,[37] yet two such ligands can coexist at the same gallium center. Again, X-ray analysis and ^{71}Ga NMR revealed that the ion pair was present both in the solid state (Figure 3) and in solution. This time, there is a clear dependence of the nature of the halide on the reaction outcome. Starting from $GaBr_3$ or GaI_3, and under the same experimental conditions, only the molecular adducts **6** and **7** were formed (see Table S2 in the Supporting Information for geometrical data).

To make the four-coordinate arrangement possible in **5**, the bulky IBiox ligands are twisted away from each other. By doing so, the CGaC angle is even more acute than in **2** (114.8° vs 120.4°), and the ClGaCl angle is larger (108.0° vs 103.3°). In contrast with phosphane adducts for which the Ga−X bonds are longer in neutral $GaEX_3$ than in cationic $GaE_2X_2^+$,[4a,8] the Ga−Cl bond lengths are longer in **2** than in the molecular adduct **1**. However, **2** does not have a NHC ligand, so the comparison is somewhat convoluted. In fact, the average Ga^1−Cl bond length is exactly the same in the two NHC adducts **5** and **1** (2.186 Å). Importantly, the Ga^1−Cl bond lengths are significantly shorter in **5** than in **2**. This underlines the fact that IBioxMe$_4$ is less electropositive than diMe-MDI (vide infra). The NCN angle is significantly different in **5** (102.5°) from that in **2** (106.7°), but this is again due to the different nature of the imidazolium rings. These angles are actually similar in **1** and **2** (∼106°), and in the more rigid IBiox derivatives **5**−**7** (∼103°), regardless of their molecular or ionic nature. In **5**, the $GaCl_4^-$ ion lies on top of the imidazolium ring as a result of ion pairing. The crystal packing of **5** shows H-bonds between the Cl atoms of both the $GaCl_2^+$ and the $GaCl_4^-$ moieties with the CH_2 and the CH_3 groups of the ligand.

Calculations were carried out to gain more insight into the factors governing the selectivity. Unlike the study that was carried out on the BH_3/NH_3 system, the large size of the molecules precludes the search for transition states, so the following discussion is restricted to minima. For large dimeric structures, the IBioxMe$_4$ series could not be computed. Table 1 shows the MP2 energies relative to the possible outcome of the reaction of L with Ga_2Cl_6 or with $GaCl_3{\cdot}THF$. The molecular adducts were treated either as separate entities (eqs 1 and 4), or as H-bonded entities (eqs 2 and 5).[8] The formation of the ion pair corresponds to eqs 3 and 6. With diMe-IMD, whether or not the solvent effect is taken into account, the thermodynamically favored process is the formation of the molecular dimer $[(\text{diMe-IMD})GaCl_3]_2$, which is in agreement with the experimental result. However, the dimer $[(\text{diMe-MDI})GaCl_3]_2$ is also energetically favored although the ion pair was isolated. One may argue that more-complex scaffolds in the solid state may reverse this order. However, we stress again that no change in structure could be observed between the solid state and the solution phase.

We then divided the addition of the two L units into two steps. Addition of one L to Ga_2Cl_6 gives rise to $LGaCl_2(\mu\text{-}Cl)GaCl_3$. Because of the low symmetry around the quadrupolar gallium nuclei, such a complex cannot be observed by ^{71}Ga NMR. However, the existence of $NH_3BH_2(\mu\text{-}H)BH_3$ could be ascertained by ^{11}B NMR, even in THF.[9] The formation of the chlorine-bridged complex is appreciably exothermic in all cases (Table 2, eq 7). It is also worthy of note that even when Ga_2Cl_6 is dissociated into $GaCl_3{\cdot}THF$, the

Scheme 6. Synthesis of $[(\text{IBioxMe}_4)_2GaCl_2]GaCl_4$ (5), $(\text{IBioxMe}_4)GaBr_3$ (6), and $(\text{IBioxMe}_4)GaI_3$ (7)

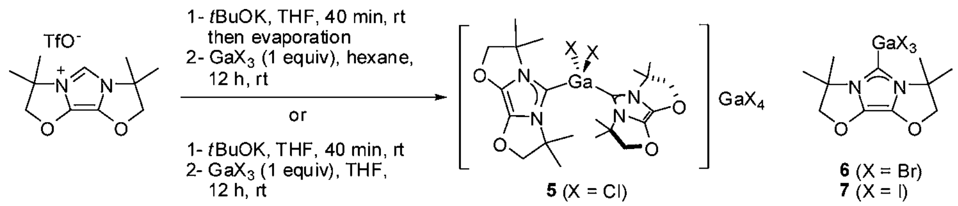

5 (X = Cl)

6 (X = Br)
7 (X = I)

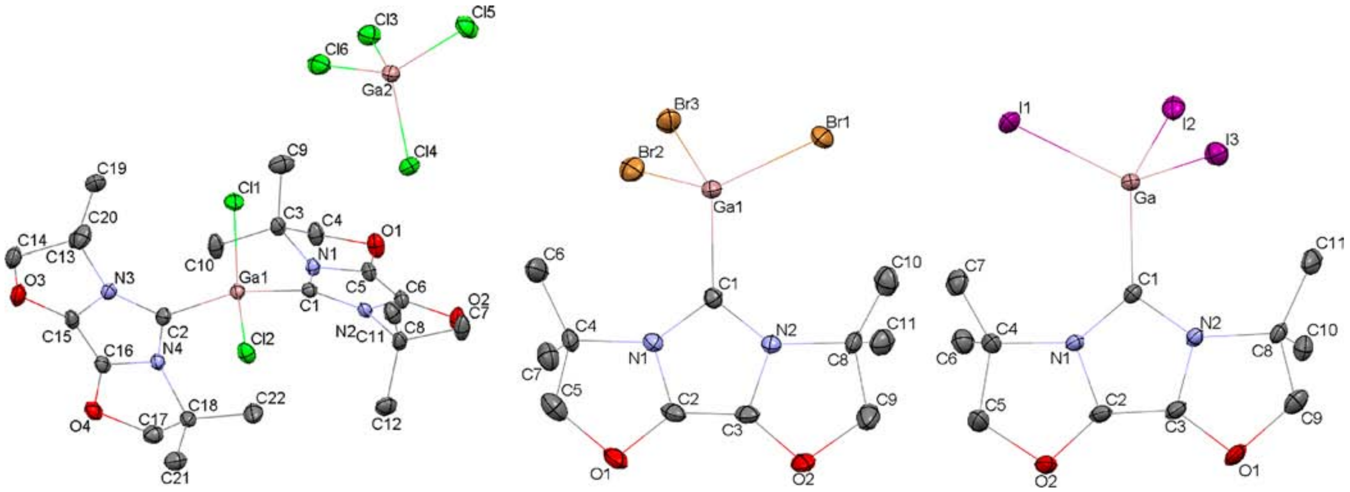

Figure 3. Crystal structure of **5**−**7** (thermal ellipsoids at 50% probability level; hydrogen atoms omitted for the sake of clarity).

Table 1. Relative Energies and Gibbs Free Energies for the Formation of Molecular Adducts and Ion Pairs at the MP2/def2-TZVPP Level

$$2\,L + Ga_2Cl_6 \longrightarrow 2\,L{\cdot}GaCl_3 \qquad (1)$$

$$2\,L + Ga_2Cl_6 \longrightarrow [L{\cdot}GaCl_3]_2 \qquad (2)$$

$$2\,L + Ga_2Cl_6 \longrightarrow [L_2GaCl_2][GaCl_4] \qquad (3)$$

$$2\,L + 2\,THF{\cdot}GaCl_3 \longrightarrow 2\,L{\cdot}GaCl_3 + 2\,THF \qquad (4)$$

$$2\,L + 2\,THF{\cdot}GaCl_3 \longrightarrow [L{\cdot}GaCl_3]_2 + 2\,THF \qquad (5)$$

$$2\,L + 2\,THF{\cdot}GaCl_3 \longrightarrow [L_2GaCl_2][GaCl_4] + 2\,THF \qquad (6)$$

L	equation	ΔE (kcal/mol)	ΔG (kcal/mol)	ΔGsolv (kcal/mol)
diMe-IMD	eq 1	−93.1	−77.5	
	eq 2	−115.1	−87.7	
	eq 3	−108.6	−79.5	
	eq 4	−27.6	−26.6	−28.4
	eq 5	−73.8	−63.4	−70.2
	eq 6	−72.1	−55.2	−66.3
diMe-MDI	eq 1	−85.3	−67.8	
	eq 2	−106.3	−75.9	
	eq 3	−102.6	−72.3	
	eq 4	−23.6	−21.7	−28.7
	eq 5	−69.3	−51.6	−73.6
	eq 6	−66.0	−48.0	−71.3

formation of the chlorine-bridged complex remains exothermic (eq 8).

Various isomers are possible for $LGaCl_2(\mu\text{-}Cl)GaCl_3$. Only the energies related to the most stable ones are given in Table 2. In fact, as shown in Figure 4, the best organization corresponds to that in which the nascent $GaCl_4^-$ ion is oriented toward the imidazolium ring, as a result of weak H-bonds ($\rho_{max} \leq 0.0078$ e Å^{-3}) and ion pairing with the ring ($\rho_{max} \leq 0.0045$ e Å^{-3}). This effect is quite strong with the diMe-IMD, the outward isomer lying 8.5 kcal/mol above the inward isomer. On the other hand, presumably because of the increased distance between the forming $GaCl_4^-$ moiety and the imidazolium ring, the inward isomer with diMe-MDI is more stable by only 1 kcal/mol. With IBioxMe$_4$, only the inward isomer converged (see Figure S1 in the Supporting Information for details).

Table 2. Relative Energies and Gibbs Free Energies for the Formation of $LGaCl_2(\mu\text{-}Cl)GaCl_3$ at the MP2/def2-TZVPP Level

$$L + Ga_2Cl_6 \longrightarrow LGaCl_2(\mu\text{-}Cl)GaCl_3 \qquad (7)$$

$$L + 2\,THF{\cdot}GaCl_3 \longrightarrow LGaCl_2(\mu\text{-}Cl)GaCl_3 + 2\,THF \qquad (8)$$

L	equation	ΔE (kcal/mol)	ΔG (kcal/mol)	ΔGsolv (kcal/mol)
diMe-IMD	eq 7	−60.7	−46.0	
	eq 8	−22.7	−21.7	−18.6
diMe-MDI	eq 7	−57.0	−41.4	
	eq 8	−19.0	−17.1	−18.7
IBioxMe$_4$	eq 7	−64.4	−48.8	
	eq 8	−26.5	−24.5	−18.0

In agreement with Bent's rule[38] and Gutmann's rule,[39] the $Ga^2{-}Cl^1$ bond distance should become longer and gain in ionic character with more electropositive ligands (Table 3). The nucleophilicity of diMe-IMD, IBioxMe$_4$, and diMe-MDI was estimated by their highest occupied molecular orbital (HOMO) level. In correlation with the average CO stretching wavenumbers,[40] the nucleophilicity increases in the following order: diMe-IMD < IBioxMe$_4$ < diMe-MDI. A nice relationship between this factor and the $Ga^2{-}Cl^1$ bond length is observed. Clearly, a more electropositive ligand weakens this bond (decreasing bond order) and increases the charge at Ga^2. It is interesting to note that while Ga^1 is the center bearing the largest charge with diMe-IMD, Ga^2 bears the largest charge with IBioxMe$_4$ and diMe-MDI. The latter promotes the most important charge transfer in the series.

Inspection of the unoccupied molecular orbitals of $LGaCl_2(\mu\text{-}Cl)GaCl_3$ is also persuasively telling (Figure 5). With L = diMe-IMD, the lowest unoccupied orbital showing a strong coefficient at gallium is LUMO+1, which is centered at Ga^1. On the other hand, LUMO+2 is centered at Ga^2. The same order is found with L = IBioxMe$_4$ (see Figure S2 in the Supporting Information). In sharp contrast, the LUMO is already centered on Ga^2 with diMe-MDI.

The second addition of L will give rise to the ion pair if it occurs at Ga^2, or to the molecular adduct if it occurs at Ga^1 (Scheme 7). Under either charge or orbital control, one expects the formation of the molecular adduct with diMe-IMD, the formation of an ion pair with diMe-MDI, and an intermediate

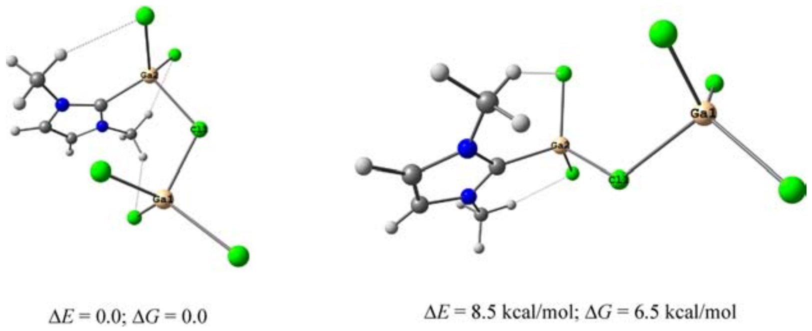

Figure 4. BP86/def2-TZVPP-optimized inward and outward isomers of (diMe-IMD)$GaCl_2(\mu\text{-}Cl)GaCl_3$ (only H-bonds <2.90 Å are represented).

Table 3. HOMO Levels, Selected Geometrical Data, Wiberg Bond Orders, and Natural Charges of BP86/def2-TZVPP Optimized $LGaCl_2(\mu\text{-}Cl)GaCl_3$

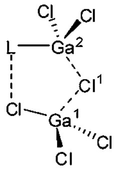

L	HOMO (eV) of L	Ga^1–Cl^1 (Å) (B.O.)[a]	Ga^2–Cl^1 (Å) (B.O.)[a]	$q(Ga^1)$[b]	$q(Ga^2)$[b]
diMe-IMD	−4.83	2.410 (0.404)	2.336 (0.494)	1.206	1.189
$IBioxMe_4$	−4.45	2.414 (0.402)	2.341 (0.488)	1.203	1.207
diMe-MDI	−3.48	2.402 (0.411)	2.371 (0.448)	1.208	1.260

[a] Wiberg natural bond order. [b] NBO partial charge.[41]

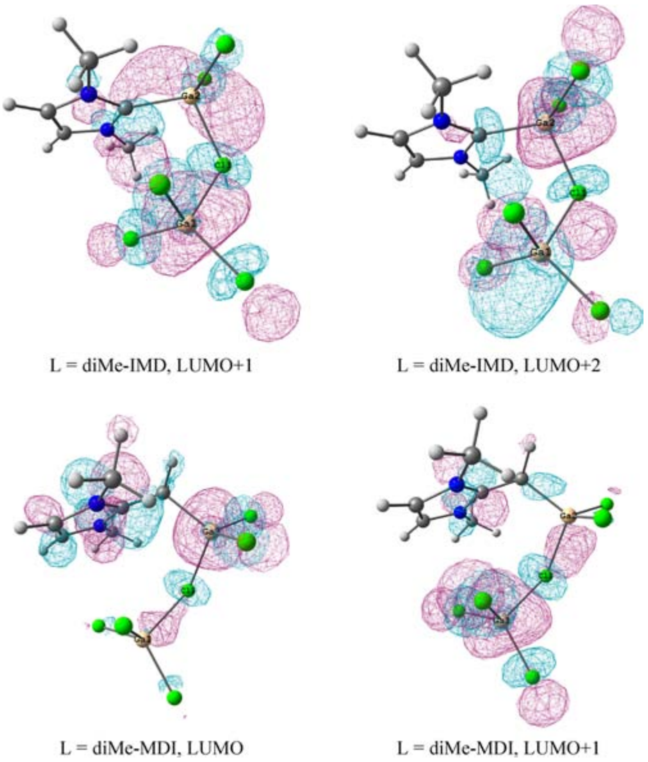

L = diMe-IMD, LUMO+1
L = diMe-IMD, LUMO+2
L = diMe-MDI, LUMO
L = diMe-MDI, LUMO+1

Figure 5. Orbital contour plot (cutoff of 0.03) of $LGaCl_2(\mu\text{-}Cl)GaCl_3$.

Scheme 7. Addition of L to $LGaCl_2(\mu\text{-}Cl)GaCl_3$

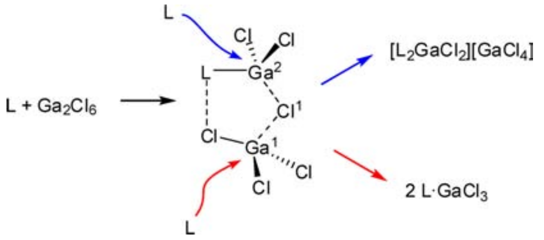

Table 4. Relative Energies and Gibbs Free Energies for $[LGaCl_2(\mu\text{-}Cl)GaCl_3][LGaCl_3]$ Adducts at the MP2/def2-TZVPP Level

$$LGaCl_2(\mu\text{-}Cl)GaCl_3 + L\cdot GaCl_3 \longrightarrow [LGaCl_2(\mu\text{-}Cl)GaCl_3][L\cdot GaCl_3] \quad (6)$$

L^{iso}	ΔE (kcal/mol)	ΔG (kcal/mol)
IMD^A	−5.9	3.7
IMD^B	−14.3	−4.3
IMD^C	−15.9	−5.5
MDI	−18.9	−5.8

case that is difficult to predict with $IBioxMe_4$. In the third case, the charges give a slight preference for Ga^2, yet Ga^1 bears a larger LUMO+2 coefficient (see Table 3 and Figure 5).

In any case, Ga^1 remains the most accessible center, the steric factor always disadvantaging Ga^2. On the basis of the work of Zhao and Shore (highlighted in Scheme 2), we wondered whether a molecular adduct could catalyze the formation of the ion pair.[9] Various isomeric scaffolds containing one (diMe-IMD)$GaCl_3$ and one (diMe-IMD)$GaCl_2(\mu\text{-}Cl)GaCl_3$ were optimized (see Table 4).

Complexes **$IMD^{A\text{-}C}$** exhibit H-bonds between the vinylic hydrogens or those of the CH_3 groups with the Cl atoms (Figure 6).[33] Only **IMD^B** and **IMD^C** can protect Ga^1 against nucleophilic attack, yet moderately. With **MDI**, thanks to the extra carbon, the binding now comprises two intermolecular H-bonds with the vinylic hydrogens (ρ_{max} = 0.0094 e Å^{-3} each) and two ion-pairing interactions between the nascent $GaCl_4^-$ ion and the two imidazolium rings (ρ_{max} = 0.0054 and 0.0045 e

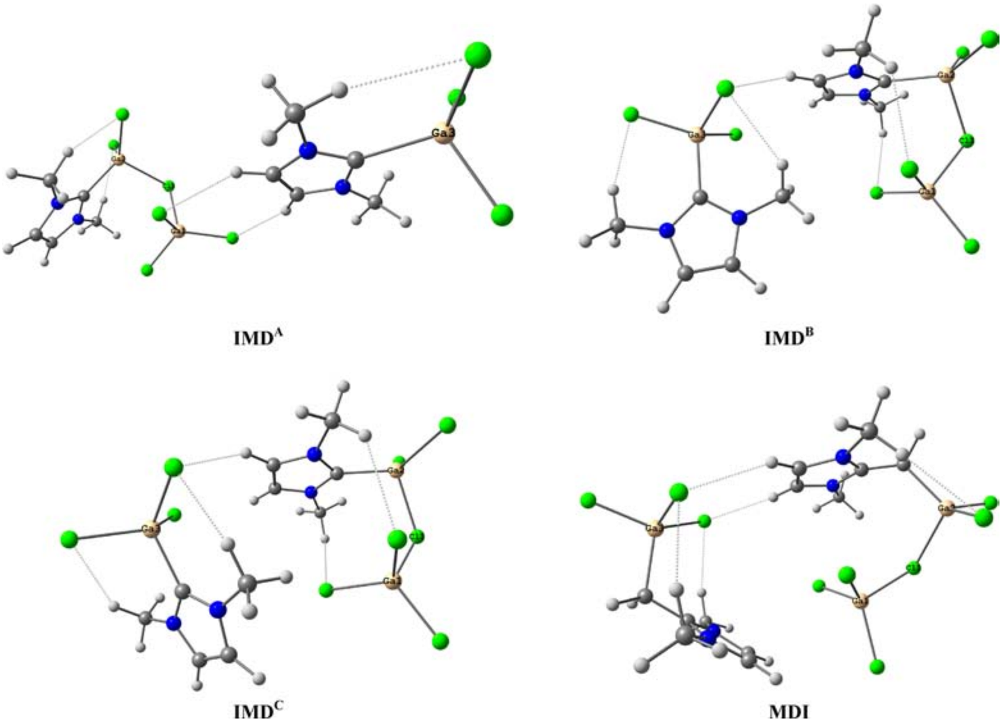

Figure 6. BP86/def2-TZVPP-optimized geometries of $[LGaCl_2(\mu\text{-}Cl)GaCl_3][LGaCl_3]$ adducts (only H-bonds <2.90 Å are represented).

Scheme 8. Addition of L to $(THF)GaCl_2(\mu\text{-}Cl)GaCl_3$

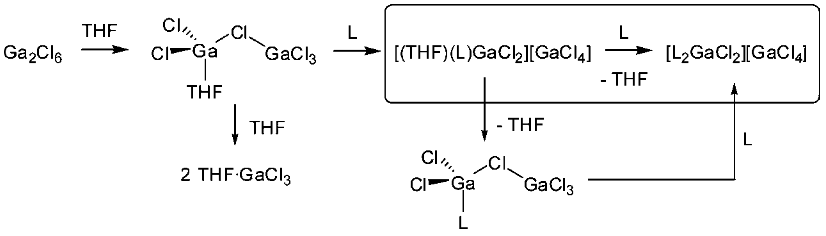

$Å^{-3}$). It results in a stabilization of 18.9 kcal/mol compared to the separated fragments (Table 4). The Ga^1 centered is far better protected in this case. It is also of note that Ga^2 keeps bearing the strongest charge (Ga^1: 1.196, Ga^2: 1.264) and the largest LUMO coefficient in this adduct.

Thus, a ligand such as diMe-MDI is perfectly suited to give rise to ion pairs, because it strongly polarizes the $Ga^2{-}Cl^1$ bond and the geometry of (diMe-MDI)$GaCl_3$ allows the protection of the most accessible gallium center (Ga^1). On the other hand, diMe-IMD is not electropositive enough and the molecular adduct cannot efficiently protect Ga^1. For ($IBioxMe_4$)$GaCl_3$, one can imagine that the methyl groups can establish H-bonds with the Cl atoms at Ga^1, which will also hinder it sterically. Pertaining to Bent's rule, $IBioxMe_4$ gives molecular adducts when reacted with $GaBr_3$ and GaI_3. Because Br and I are less electronegative than Cl, there is less p character concentrated in the Ga−Br and Ga−I bonds, so their cleavage will be more difficult. Only a very nucleophilic ligand such as diMe-MDI will be able to do so.

The above mechanistic proposal relies on the cleavage of Ga_2Cl_6 into $LGaCl_2(\mu\text{-}Cl)GaCl_3$ as first step. In THF, Ga_2Cl_6 is actually already cleaved into $GaCl_3{\cdot}THF$, yet a small amount of $GaCl_3$ could form $(THF)GaCl_2(\mu\text{-}Cl)GaCl_3$ (Scheme 8). This species could react with the carbon-based ligand L to give $[(THF)(L)GaCl_2][GaCl_4]$. Unlike indium and thallium, gallium is reluctant to reach coordination numbers higher than 4. That means that the transformation of $[(THF)(L)GaCl_2][GaCl_4]$ into the final product $[L_2GaCl_2][GaCl_4]$ would proceed in a dissociative fashion, leading to $LGaCl_2(\mu\text{-}Cl)GaCl_3$. Thus, this possible pathway is finally equivalent to the one previously discussed.

■ CONCLUSION

This study shows that the reaction of monodentate carbon-based ligands with gallium(III) halides can give rise to ionic 1:1 adducts of type $[L_2GaX_2][GaX_4]$. The formation of these rare nonchelated assemblies is favored by strongly donor ligands. Calculations suggest that the formation of these species is due to the polarization of the $Ga^2{-}X^1$ bond in $LGa^2X_2(\mu\text{-}X^1)Ga^1X_3$, an intermediate that is formed after addition of one ligand unit onto dimeric or monomeric GaX_3. Consistent with the formation mechanism of the diammoniate of diborane, it is also possible that a catalytic amount of molecular $L{\cdot}GaX_3$ directs the addition of the second ligand unit onto the most electropositive gallium center.

■ ASSOCIATED CONTENT

Ⓢ Supporting Information

Crystallographic information files (CIFs). Coordinates and energies of the computed species. This material is available free of charge via the Internet at http://pubs.acs.org.

■ AUTHOR INFORMATION

Corresponding Author

*Tel.: +33 169 153 931. Fax: +33 169 154 747. E-mail: vincent.gandon@u-psud.fr..

Notes

The authors declare no competing financial interest.

■ ACKNOWLEDGMENTS

We thank UPS (Chaire d'Excellence) and CNRS for financial support. V.G. is a member of the Institut Universitaire de France (IUF). We warmly thank Prof. Tom Morton for helpful discussions and Prof. David Aitken for proofreading. We used the computing facility of the CRIHAN (Project No. 2006-013).

■ REFERENCES

(1) (a) Dagorne, S.; Atwood, D. A. *Chem. Rev.* **2008**, *108*, 4037. (b) Davydova, E. I.; Sevastianova, T. N.; Suronov, A. V.; Timoshkin, A. Y. *Coord. Chem. Rev.* **2010**, *254*, 2031. (c) Piers, W. E.; Bourke, S. C.; Conroy, K. D. *Angew. Chem., Int. Ed.* **2005**, *44*, 5016. (d) *The Group 13 Metals Aluminum, Gallium, Indium and Thallium: Chemical Patterns and Peculiarities*; Aldridge, S., Downs, A. J., Eds.; John Wiley & Sons: New York, 2011.

(2) Stock, A.; Kuss, E. *Ber. Dtsch. Chem. Ges.* **1923**, *56*, 789.

(3) (a) Parry, R. W.; Schultz, D. R.; Girardot, P. R. *J. Am. Chem. Soc.* **1958**, *80*, 1. (b) Schultz, D. R.; Parry, R. W. *J. Am. Chem. Soc.* **1958**, *80*, 4. (c) Shore, S. G.; Parry, R. W. *J. Am. Chem. Soc.* **1958**, *80*, 8. (d) Shore, S. G.; Parry, R. W. *J. Am. Chem. Soc.* **1958**, *80*, 12. (e) Parry, R. W.; Shore, S. G. *J. Am. Chem. Soc.* **1958**, *80*, 15. (f) Shore, S. G.; Girardot, P. R.; Parry, R. W. *J. Am. Chem. Soc.* **1958**, *80*, 20. (g) Parry, R. W.; Kodama, G.; Schultz, D. R. *J. Am. Chem. Soc.* **1958**, *80*, 24.

(4) (a) Cheng, F.; Hector, A. L.; Levason, W.; Reid, G.; Webster, M.; Zhang, W. *Inorg. Chem.* **2007**, *46*, 7215. (b) Gurnani, C.; Levason, W.; Ratnani, R.; Reid, G.; Webster, M. *Dalton Trans.* **2008**, 6274. (c) Cheng, F.; Friend, S. I.; Hector, A. L.; Levason, W.; Reid, G.; Webster, M.; Zhang, W. *Inorg. Chem.* **2008**, *47*, 9691.

(5) (a) Means, N. C.; Mitchell Means, C.; Bott, S. G.; Atwood, J. L. *Inorg. Chem..* **1987**, *26*, 1466. (b) Schick, G.; Loew, A.; Nieger, M.; Airola, K.; Niecke, E. *Chem. Ber.* **1996**, *129*, 911.

(6) Cheng, F.; Codgbrook, H. L.; Hector, A. L.; Levason, W.; Reid, G.; Webster, M.; Zhang, W. *Polyhedron* **2007**, *26*, 4147.

(7) (a) Kratz, F.; Nuber, B.; Weiss, J.; Keppler, B. K. *Polyhedron* **1992**, *11*, 487. (b) Cortes-Llamas, S. A.; García-Hernández, Z.; Rufino-Felipe, E.; López-Cardoso, M.; Muñoz-Hernández, M.-A. *Inorg. Chim. Acta* **2010**, *363*, 3959.

(8) Trinh, C.; Bodensteiner, M.; Virovets, A. V.; Peresypkina, E. V.; Scheer, M.; Matveev, S. M.; Timoshkin, A. Y. *Polyhedron* **2010**, *29*, 414.

(9) Chen, X.; Bao, X.; Zhao, J.-C.; Shore, S. G. *J. Am. Chem. Soc.* **2011**, *133*, 14172.

(10) (a) Ueng, S.-H; Makhlouf Brahmi, M.; Derat, E.; Fensterbank, L.; Lacôte, E.; Malacria, M.; Curran, D. P. *J. Am. Chem. Soc.* **2008**, *130*, 10082. (b) Curran, D. P.; Solovyev, A.; Makhlouf Brahmi, M.; Fensterbank, L.; Malacria, M.; Lacôte, E. *Angew. Chem., Int. Ed.* **2011**, *50*, 10294. (c) Tehfe, M.-A.; Monot, J.; Malacria, M.; Fensterbank, L.; Fouassier, J.-P.; Curran, D. P.; Lacôte, E.; Lalevée, J. *ACS Macro Lett.* **2012**, *1*, 92.

(11) (a) Zhou, H.; Campbell, J. E.; Nguyen, S. T. *Org. Lett.* **2001**, *3*, 2229. (b) Buffet, J.-C.; Okuda, J.; Arnold, P. L. *Inorg. Chem.* **2010**, *49*, 419. (c) Suzuki, T.; Atsumi, J.-i.; Sengoku, T.; Takahashi, M.; Yoda, H. *J. Organomet. Chem.* **2010**, *695*, 128. (d) Li, Z.; Plancq, B.; Ollevier, T. *Chem.—Eur. J.* **2012**, *18*, 3144. (e) Qiu, R.; Yin, S.; Song, X.; Meng, Z.; Qiu, Y.; Tan, N.; Xu, X.; Luo, S.; Dai, F.-R.; Au, C.-T.; Wong, W.-Y *Dalton Trans.* **2011**, *40*, 9482. (f) Lamberti, M.; D'Auria, I.; Mazzeo, M.; Milione, S.; Bertolasi, V.; Pappalardo, D. *Organometallics* **2012**, *31*, 5551. (g) Bakewell, C.; Platel, R. H.; Cary, S. K.; Hubbard, S. M.; Roaf, J. M.; Levine, A. C.; White, A. J. P.; Long, N. J.; Haaf, M.; Williams, C. K. *Organometallics* **2012**, *31*, 4729. (h) Tian, D.; Liu, B.; Zhang, L.; Wang, X.; Zhang, W.; Han, L.; Park, D.-W. *J. Ind. Eng. Chem.* **2012**, *18*, 1332.

(12) (a) Power, P. P. *Nature* **2010**, *463*, 171. (b) Summerscales, O. T.; Fettinger, J. C.; Power, P. P. *J. Am. Chem. Soc.* **2011**, *133*, 11960. (c) Power, P. P. *Acc. Chem. Res.* **2011**, *44*, 627.

(13) (a) Bonyhady, S. J.; Collis, D.; Frenking, G.; Holzmann, N.; Jones, C.; Stasch, A. *Nat. Chem.* **2010**, *2*, 865. (b) Holzmann, N.; Stasch, A.; Jones, C.; Frenking, G. *Chem.—Eur. J.* **2011**, *17*, 13517.

(14) Zhuo, L.-G.; Zhang, J.-J.; Yu, Z.-X. *J. Org. Chem.* **2012**, DOI: dx.doi.org/10.1021/jo301471w.

(15) (a) Evans, D. A.; Chapman, K. T.; Bisaha, J. *J. Am. Chem. Soc.* **1988**, *110*, 1238. (b) Tietze, L. F.; Schuffenhauer, A.; Schreiner, P. R. *J. Am. Chem. Soc.* **1998**, *120*, 7952. (c) Lam, Y.-h.; Cheong, P. H.-Y.; Blasco Mata, J. M.; Stanway, S. J.; Gouverneur, V.; Houk, K. N. *J. Am. Chem. Soc.* **2009**, *131*, 1947.

(16) Tang, S.; Monot, J.; El-Hellani, A.; Michelet, B.; Guillot, R.; Bour, C.; Gandon, V. *Chem.—Eur. J.* **2012**, *18*, 10239.

(17) Cambridge Crystallographic Data Centre (CCDC) registry numbers: **1** (904827), **2** (904828), **5** (904829), **6** (904830), **7** (904831).

(18) Fürstner, A.; Alcarazo, M.; Goddard, R.; Lehmann, C. W. *Angew. Chem., Int. Ed.* **2008**, *47*, 3210.

(19) Altenhoff, G.; Goddard, R.; Lehmann, C. W.; Glorius, F. *J. Am. Chem. Soc.* **2004**, *126*, 15195.

(20) Frisch, M. J. et al.; Gaussian 03, Revision C.02; Gaussian, Inc.: Wallingford, CT, 2004.

(21) (a) Becke, A. D. *Phys. Rev. A* **1988**, *38*, 3098. (b) Perdew, J. P. *Phys. Rev. B* **1986**, *33*, 8822.

(22) Weigend, F.; Ahlrichs, R. *Phys. Chem. Chem. Phys.* **2005**, *7*, 3297.

(23) (a) Boys, S. F.; Bernardi, F. *Mol. Phys.* **1970**, *19*, 553. (b) Simon, S.; Duran, M.; Dannenberg, J. J. *J. Chem. Phys.* **1996**, *105*, 11024.

(24) Tomasi, J.; Mennucci, B.; Cammi, R. *Chem. Rev.* **2005**, *105*, 2999.

(25) (a) Møller, Chr.; Plesset, M. S. *Phys. Rev.* **1934**, *46*, 618. (b) Binkley, J. S.; Pople, J. A. *Int. J. Quantum Chem.* **1975**, *9*, 229.

(26) Cheng, F.; Codgbrook, H. L.; Hector, A. L.; Levason, W.; Reid, G.; Webster, M.; Zhang, W. *Polyhedron* **2007**, *26*, 4147.

(27) (a) Carmalt, C. J.; Cowley, A. H. *Adv. Inorg. Chem.* **2000**, *50*, 1. (b) Carmalt, C. J. Main group carbenes. In *Encyclopedia of Inorganic Chemistry*; John Wiley & Sons: Chichester, U.K., 2006 (DOI: 10.1002/9781119951438.eibc0272).

(28) (a) Stasch, A.; Singh, S.; Roesky, H. W.; Noltemeyer, M.; Schmidt, H.-G. *Eur. J. Inorg. Chem.* **2004**, 4052. (b) Ghadwal, R. S.; Roesky, H. W.; Herbst-Irmer, R.; Jones, P. G. *Z. Anorg. Allg. Chem.* **2009**, *635*, 431.

(29) For (NHC)GaX_3, X = halide, see refs 16, 28a, and: (a) Marion, N.; Escudo-Adán, E. C.; Benet-Buchholz, J.; Stevens, E. D.; Fensterbank, L.; Malacria, M.; Nolan, S. P. *Organometallics* **2007**, *26*, 3256. (b) Ball, G. E.; Cole, M. L.; McKay, A. I. *Dalton Trans.* **2012**, *41*, 946. X = H: (c) Francis, M. D.; Hibbs, D. E.; Hursthouse, M. B.; Jones, C.; Smithies, N. A. *J. Chem. Soc., Dalton Trans.* **1998**, 3249. X = Me: (d) Li, X.-W.; Su, J.; Robinson, G. H. *Chem. Commun.* **1996**, 2683. Mixed species: (e) Cole, M. L.; Furfari, S. K.; Kloth, M. *J. Organomet. Chem.* **2009**, *694*, 2934. (f) Horeglad, P.; Szczepaniak, G.; Dranka, M.; Zachara, J. *Chem. Commun.* **2012**, 1171. (g) Quillian, B.; Wei, P.; Wannere, C. S.; Schleyer, P. v. R.; Robinson, G. H. *J. Am. Chem. Soc.* **2009**, *131*, 3168. (h) Wang, Y.; Robinson, G. H. *Inorg. Chem.* **2011**, *50*, 12326.

(30) (a) Cowley, A. H.; Gabbaï, F. P.; Carrano, C. J.; Mokry, L. M.; Bond, M. R.; Bertrand, G. *Angew. Chem., Int. Ed. Engl.* **1994**, *33*, 578. (b) Masuda, J. D.; Martin, D.; Lyon-Saunier, C.; Baceiredo, A.;

Gornitzka, H.; Donnadieu, B.; Bertrand, G. *Chem.—Asian J.* **2007**, *2*, 178.

(31) (a) Black, S. J.; Hibbs, D. E.; Hursthouse, M. B.; Jones, C.; Abdul Malik, K. M.; Smithies, N. A. *J. Chem. Soc., Dalton Trans.* **1997**, 4313. (b) Abernethy, C. D.; Cole, M. L.; Jones, C. *Organometallics* **2000**, *19*, 4852. (c) Baker, R. J.; Davies, A. J.; Jones, C.; Kloh, M. *J. Organomet. Chem.* **2002**, *656*, 203.

(32) Cole, M. L.; Davies, A. J.; Jones, C. *J. Chem. Soc., Dalton Trans.* **2001**, 2451.

(33) For imidazolium−anion interactions, see: (a) Hunt, P. A.; Gould, I. R. *J. Phys. Chem. A* **2006**, *110*, 2269. (b) Spence, G. T.; Serpell, C. J.; Sardinha, J.; Costa, P. J.; Félix, V.; Beer, P. D. *Chem.—Eur. J.* **2011**, *17*, 12955.

(34) Kuhn, N.; Al-Sheikh, A. *Coord. Chem. Rev.* **2005**, *249*, 829.

(35) (a) Xue, H.; Tong, Z.-F.; Wei, F.-Y.; Qing, S.-G. *C. R. Chim.* **2008**, *11*, 90. (b) Felix, A. M.; Dickie, D. A.; Horne, I. S.; Page, G.; Kemp, R. A. *Inorg. Chem.* **2012**, *51*, 4650.

(36) Scholz, S.; Lerner, H.-W.; Bolte, M. *Acta Crystallogr., Sect. E: Struct. Rep. Online* **2002**, *E58*, m586.

(37) Values obtained from our X-ray structures (including hydrogens) at 2.00 Å, using SambVca: http://www.molnac.unisa.it/OMtools/sambvca.php. For information about the percent buried volume, see: (a) Poater, A.; Cosenza, B.; Correa, A.; Giudice, S.; Ragone, F.; Scarano, V.; Cavallo, L. *Eur. J. Inorg.* **2009**, 1759. (b) Clavier, H.; Nolan, S. P. *Chem. Commun.* **2010**, *46*, 841.

(38) (a) Bent, H. A. *J. Chem. Educ.* **1960**, *37*, 616. (b) Bent, H. A. *Chem. Rev.* **1961**, *61*, 275. (c) Huheey, J. E. *Inorg. Chem.* **1981**, *20*, 4033. (d) Jonas, V.; Boehme, C.; Frenking, G. *Inorg. Chem.* **1996**, *35*, 2097.

(39) (a) Gutmann, V. *Coord. Chem. Rev.* **1975**, *15*, 207. (b) Gutmann, V. *The Donor−Acceptor Approach to Molecular Interactions*; Plenum Press: New York, 1977. (c) Jensen, W. B. *The Lewis Acid−Base Concepts: An Overview*; Wiley and Sons: New York, 1980. (d) Denmark, S. E.; Beutner, G. L. *Angew. Chem., Int. Ed.* **2008**, *47*, 1560.

(40) For diMe-IMD, see: (a) Gusev, D. G. *Organometallics* **2009**, *28*, 763. (b) Gusev, D. G. *Organometallics* **2009**, *28*, 6458. (c) Khramov, D. M.; Lynch, V. M.; Bielawski, C. W. *Organometallics* **2007**, *26*, 6042. For IBioxMe$_4$, see ref 19 and: (d) Dröge, T.; Glorius, F. *Angew. Chem., Int. Ed.* **2010**, *49*, 6940. (e) Altenhoff, G.; Goddard, R.; Lehmann, C. W.; Glorius, F. *Angew. Chem., Int. Ed.* **2003**, *42*, 3690. (f) For diMe-MDI, see ref 18.

(41) (a) Foster, J. P.; Weinhold, F. *J. Am. Chem. Soc.* **1980**, *102*, 7211. (b) Weinhold, F.; Carpenter, J. E. In *The Structure of Small Molecules and Ions*; Naaman, R., Vager, Z., Eds.; Plenum Press: New York, 1988; p 227.